Science Advances

AAAS

advances.sciencemag.org/cgi/content/full/3/5/e1700015/DC1

Supplementary Materials for

Ultrastretchable, transparent triboelectric nanogenerator as electronic skin for biomechanical energy harvesting and tactile sensing

Xiong Pu, Mengmeng Liu, Xiangyu Chen, Jiangman Sun, Chunhua Du, Yang Zhang, Junyi Zhai, Weiguo Hu, Zhong Lin Wang

Published 31 May 2017, *Sci. Adv.* **3**, e1700015 (2017)
DOI: 10.1126/sciadv.1700015

The PDF file includes:

Other Supplementary Material for this manuscript includes the following:

(available at advances.sciencemag.org/cgi/content/full/3/5/e1700015/DC1)

- movie S1 (.wmv format). Hand-tapping energy harvesting of a VHB-STENG at initial state.
- movie S2 (.wmv format). Hand-tapping energy harvesting of a VHB-STENG at stretched state.
- movie S3 (.wmv format). Powering an LCD screen by a transparent VHB-STENG.
- movie S4 (.wmv format). Powering an electronic watch with the energy converted from hand tapping by a PDMS-STENG.

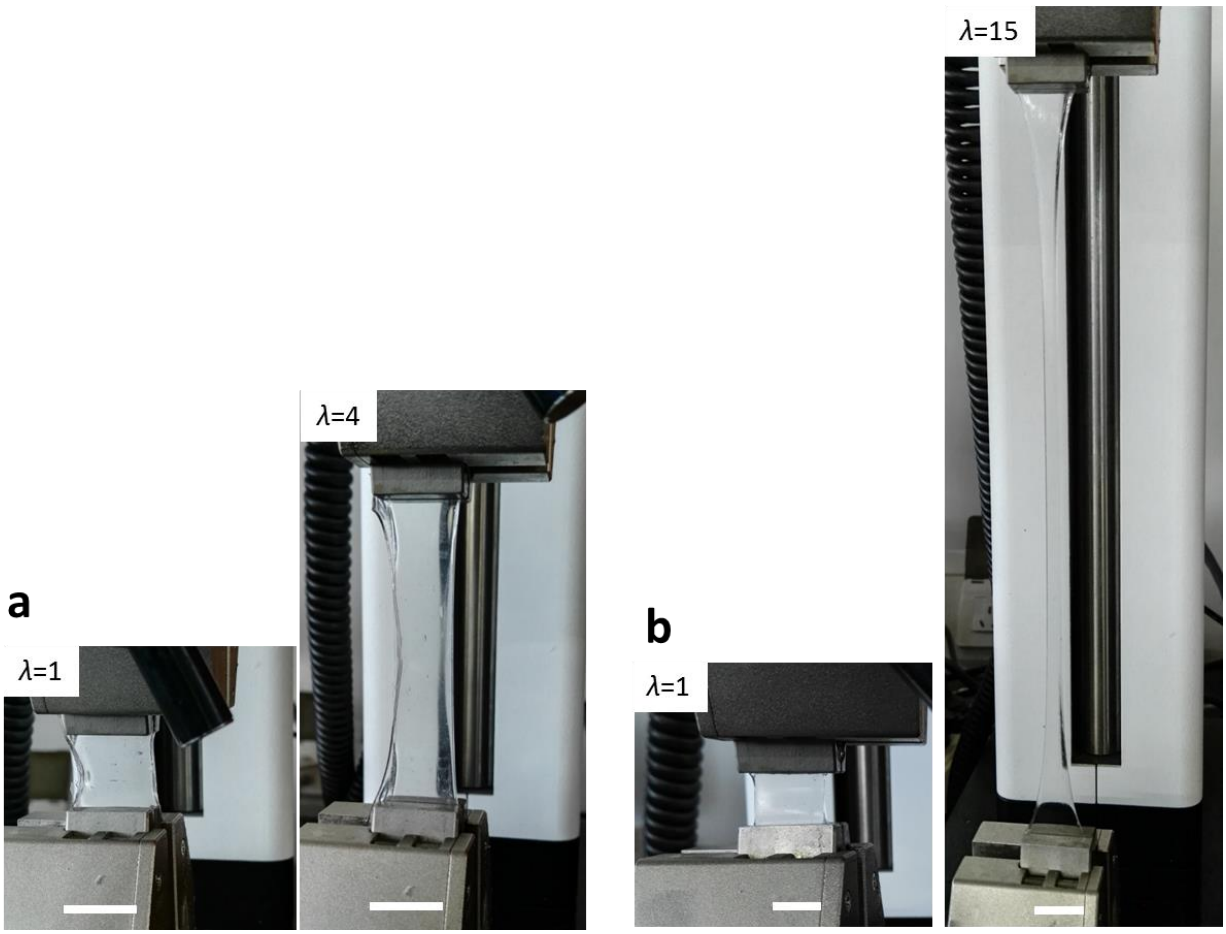

fig. S1. The images of the stretchable PDMS-STENG and hydrogel. The photo of (**a**) a PDMS-STENG at stretch λ=1 and λ=4, and (**b**) a PAAm-LiCl hydrogel at stretch λ=1 and λ=15. The scale bar is 15 mm in (a) and 10 mm in (b).

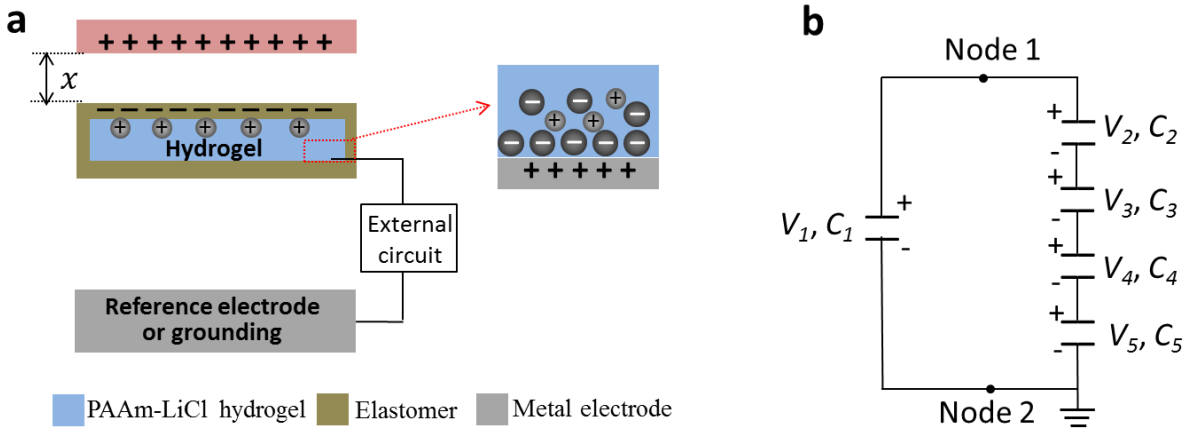

fig. S2. The explanation of the working mechanism of the STENG. (**a**) Schematic illustration of a STENG at single-electrode mode, and (**b**) corresponding equivalent circuit at open-circuit condition. The STENG is equivalent to a circuit consisting of a series of capacitors:

C_1 is the capacitance between the moving dielectric film and the reference electrode,

C_2 is the capacitance between the moving dielectric film and the elastomer film,

C_3 is the capacitance between the elastomer film and the hydrogel,

C_4 is the electrical double layer (EDL) capacitance at the hydrogel/metal wire interface, and

C_5 is the capacitance between the metal wire and the reference electrode.

As both the ratio of the area of capacitor C_3 (3×4 cm^2) to the thickness of the elastomer film (90~130 μm), and the ratio of the area of EDL capacitor C_4 (on the order of ~10 mm^2) to the thickness of EDL (on the order of ~1 nm) are large, the capacitances of C_3 and C_4 are very large. Therefore the voltage drop across the capacitor C_3 and C_4 is low and negligible. *(10, 37, 38)* Therefore, it can be estimated that

$$V_1 = V_2 + V_5 \quad (1)$$

At node 1, the charge quantity is σA, where σ is the charge density generated at the surface of the elastomer film and the moving dielectric film, and A is the contacting area. At node 2, the charge quantity is 0 at open-circuit condition. Then

$$C_1V_1 + C_2V_2 = \sigma A \tag{2}$$

$$-C_1V_1 - C_5V_5 = 0 \tag{3}$$

Thus, at open-circuit condition the V_5 (i.e. the V_{OC} of the STENG) can be obtained as

$$V_5 = V_{OC} = \frac{-\sigma A C_1}{C_1C_5 + C_2C_5 + C_1C_2} \tag{4}$$

Meanwhile, the capacitance of the STENG can also be estimated to be the following equation, considering that C_3 and C_4 are both very large

$$C_o = C_5 + \frac{C_1C_2}{C_1 + C_2} \tag{5}$$

Also, the STENG follows the relationship that: (*36*, *38*)

$$Q_{SC} = V_{OC}C_o \tag{6}$$

Therefore, at short-circuit condition

$$Q_{SC} = \frac{-\sigma A C_1}{C_1 + C_2} \tag{7}$$

When the moving dielectric film is moving far away (the distance between the dielectric and elastomer film x is approaching to infinity), both the C_1 and C_2 is approaching to zero at the same rate, and the ratio C_1/C_2 is approaching to 1, and C_o is approaching to C_5. (*38*) Therefore, following equations can be estimated when x is infinity:

$$Q_{SC} = \frac{-\sigma A}{2} \tag{8}$$

$$V_{OC} = \frac{-\sigma A}{2C_o} \tag{9}$$

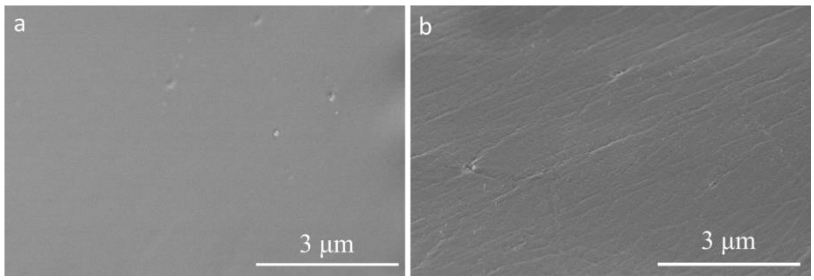

fig. S3. The scanning electron microscopy image of the surface of PDMS and VHB.

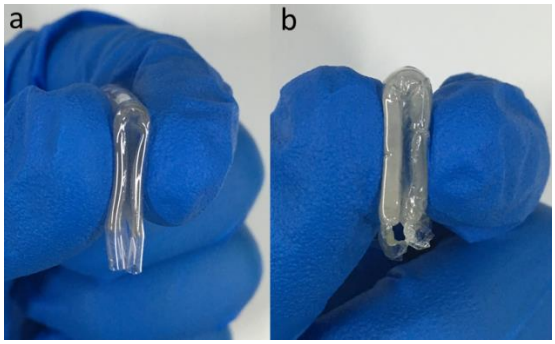

fig. S4. The images of the PDMS-STENG and VHB-STENG folded completely.

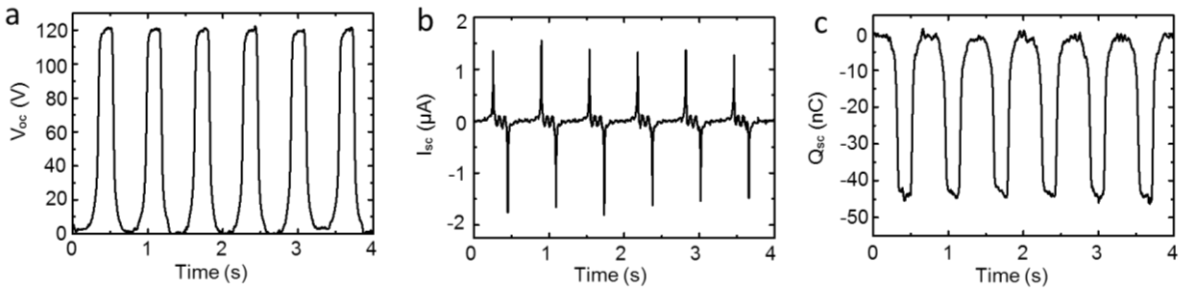

fig. S5. The output characteristics of a VHB-STENG at single-electrode mode. (**a**) The open-circuit voltage V_{oc}, (**b**) short-circuit current I_{sc} and (**c**) short-circuit charge quantity Q_{sc} of a VHB-STENG with contact-separation motion relative to a latex film.

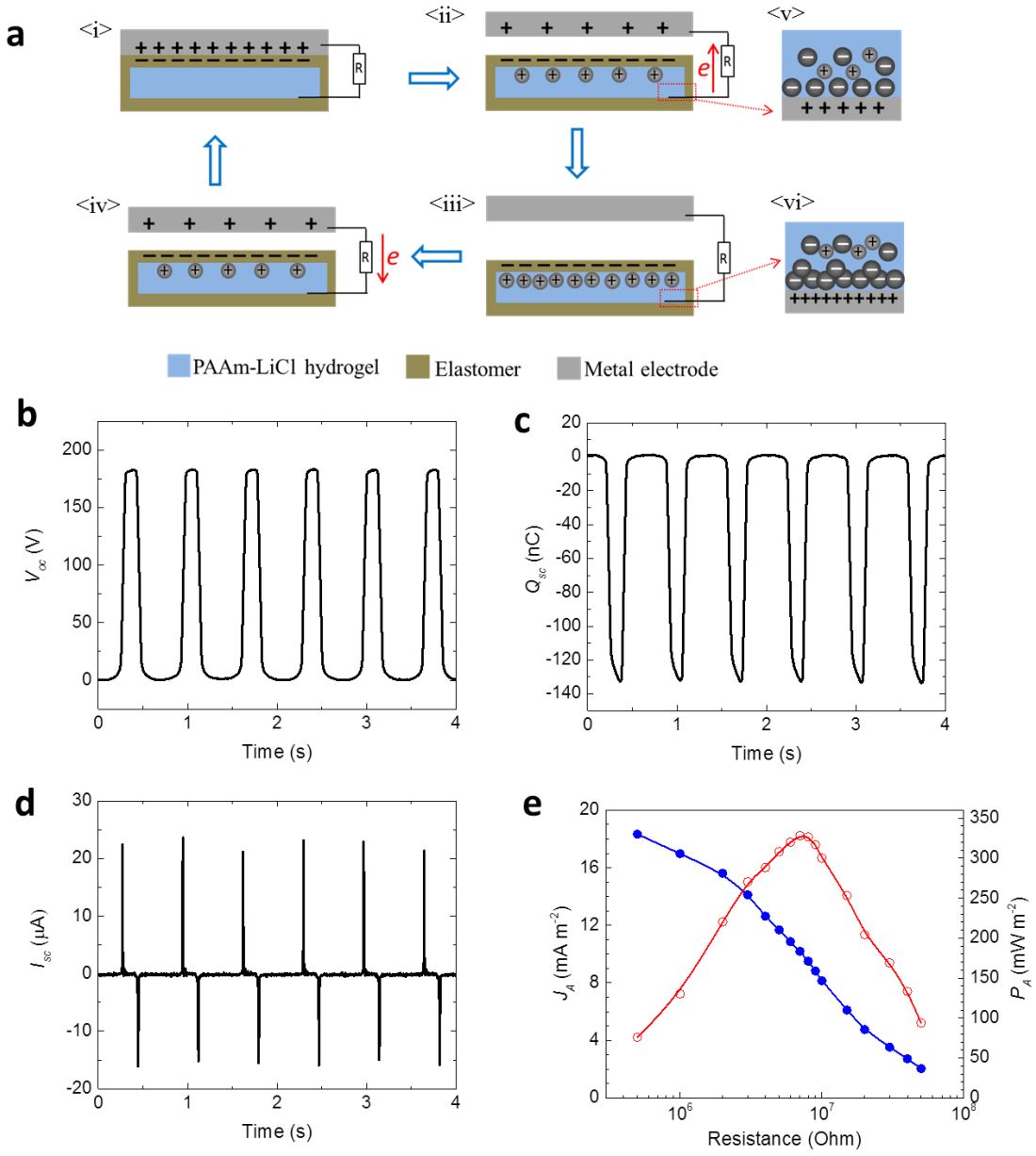

fig. S6. The working mechanism and output characteristics of the STENG at two-electrode mode. (**a**) The scheme of the working mechanism of the STENG at two-electrode mode. Once the metal film (for example Al) contacts with the elastomer film (for example PDMS), electrification happens at the interface (<i>), resulting in the formation of positive and negative charges at the surface of the Al and PDMS, respectively, because Al is more tribo-positive and

tending to lose electrons comparing with PDMS. When the two surfaces are separating and moving away, the static charges on the surface of the insulating PDMS will induce the movement of the ions in the ionic hydrogel to balance the static charges, forming a layer of excessive positive ions (<ii>) at the PDMS/hydrogel interface. Meanwhile, electrons flow from the Al film to the hydrogel/metal wire interface through the external circuits, forming an electrical double layer as depicted in <v>. The electron flux will be stopped until all the static charges in the elastomer film are screened and the Al film is neutralized (<iii>). If the Al film is approaching back to PDMS film, the whole process will be reversed and an electron flux with the opposite direction will transfer from the Al film to the hydrogel/metal wire interface through the external load (<iv>). By repeating the contact-separation movement between the object and the STENG, alternative current will be generated. . (**b**) The open-circuit voltage V_{oc}, (**c**) short-circuit charge quantity Q_{sc} and (**d**) short-circuit current I_{sc} of a PDMS-STENG working at two-electrode mode. (**e**) The variation of the output current density and power density of the PDMS-STENG with the external loading resistance.

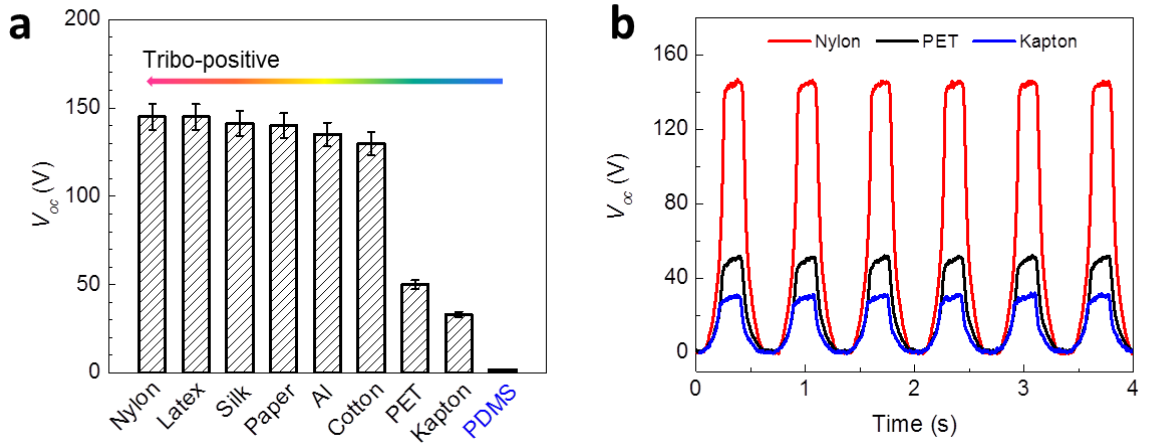

fig. S7. Material choices of the PDMS-STENG. (**a**) The summarized peak amplitude of V_{oc} and (**b**) three representative V_{oc} profiles of a PDMS-STENG with relative contact-separation motion to different materials at single –electrode mode.

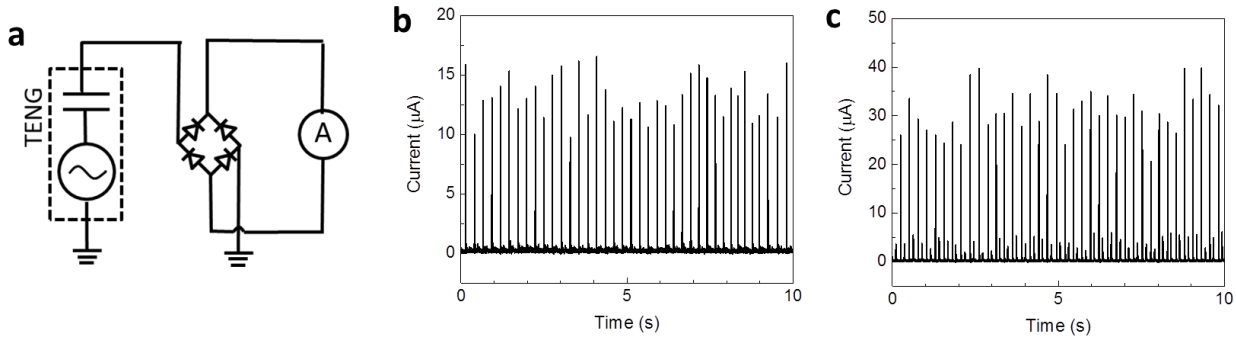

fig. S8. Rectified current output of the STENG by hand tapping. (**a**) The equivalent circuit measuring the rectified short-circuit current of the STENG at single-electrode mode. The output I_{sc} of a PDMS-STENG at single-electrode mode pressed by (**b**) a hand with latex glove and (**c**) a bare hand.

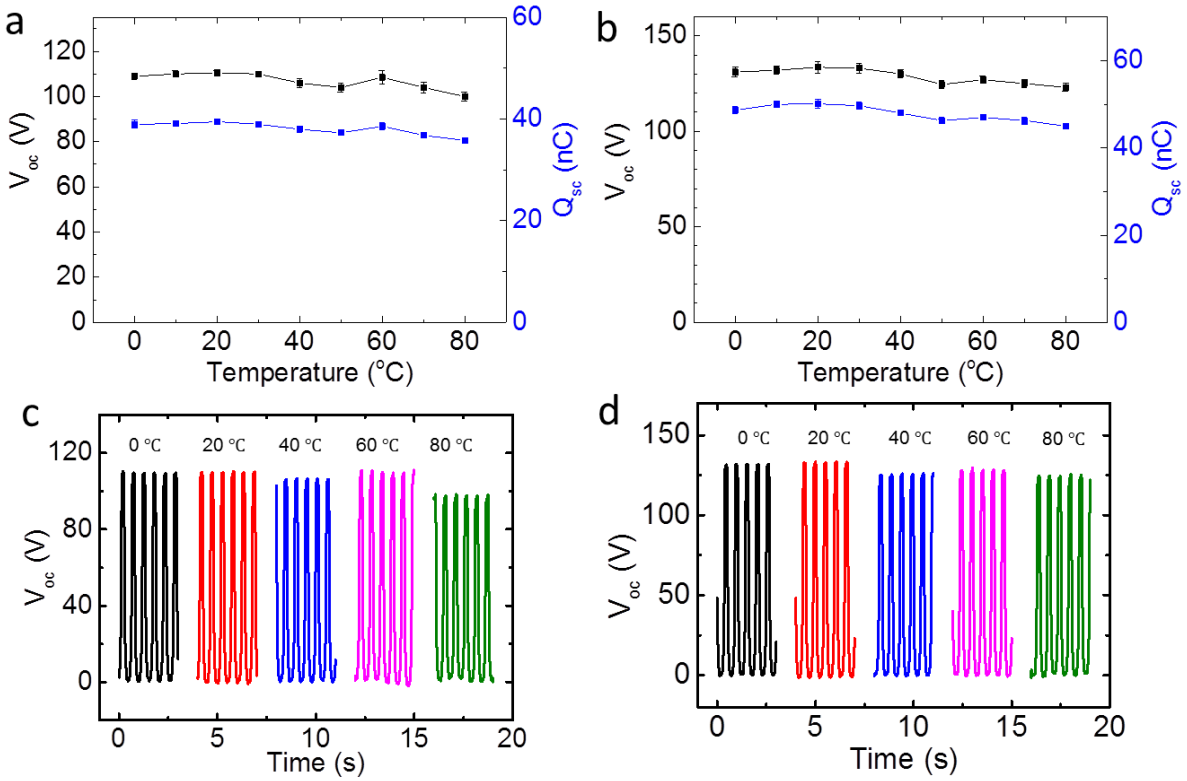

fig. S9. Temperature effect on the performances of the STENG. Summarized V_{oc} and Q_{sc} of (**a**) VHB-STENG and (**b**) PDMS-STENG measured at different temperatures with contact-separation to a latex film. Typical output V_{oc} profiles of (**c**) the VHB-STENG and (**d**) PDMS-STENG at different temperatures.

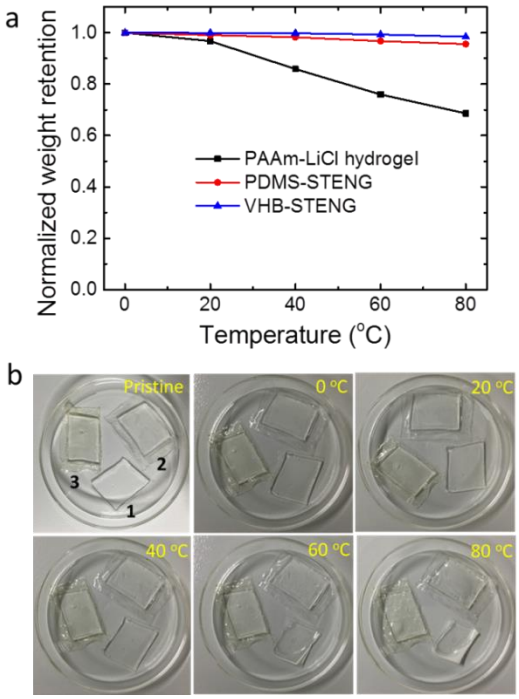

fig. S10. Thermal durability of the STENG. (**a**)Weight retention of the bare PAAm-LiCl hydrogel, PDMS-STENG, and VHB-STENG, after the storage at 0~80 ºC for 30 min. consecutively. (**b**) The photos of the bare PAAm-LiCl hydrogel (sample 1), PDMS-STENG (sample 2), and VHB-STENG (sample 3), before and after the storage at 0~80 ºC for 30 min.

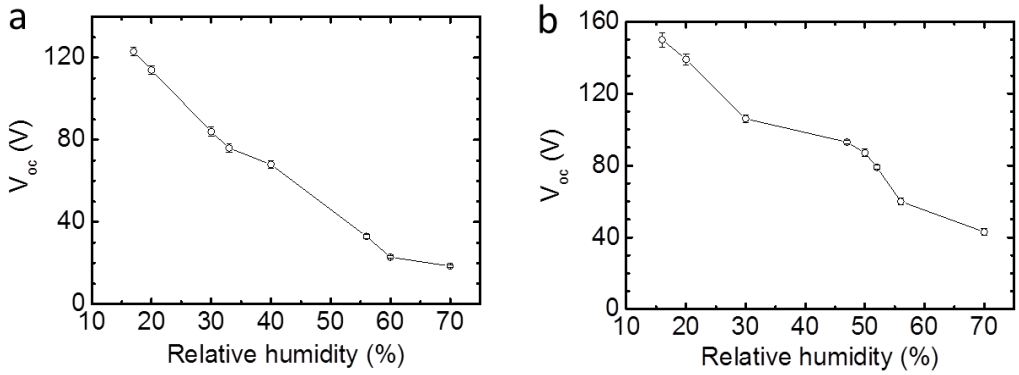

fig. S11. Humidity effect on the performances of the STENG. Summarized V_{oc} of (**a**) VHB-STENG and (**b**) PDMS-STENG measured at different relative humidity with contact-separation to a latex film.

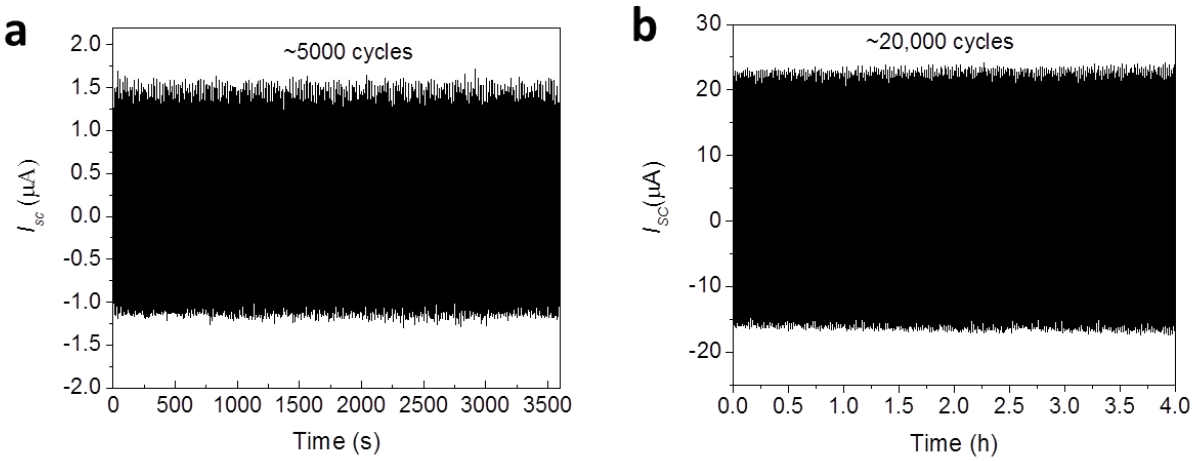

fig. S12. The durability of the STENG. The output I_{sc} of a PDMS-STENG (**a**) at single-electrode mode and (**b**) at two-electrode mode for elongated motion cycles.

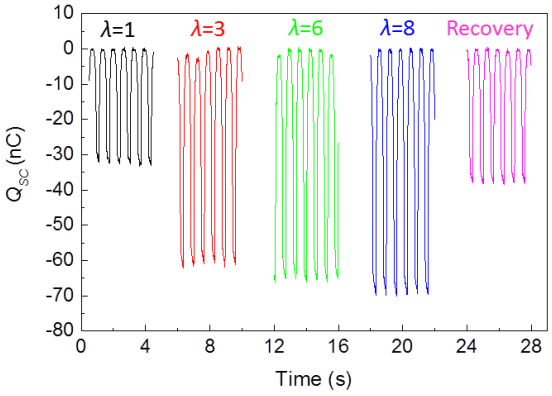

fig. S13. The Q_{SC} of a VHB-STENG at initial state and different stretched states.

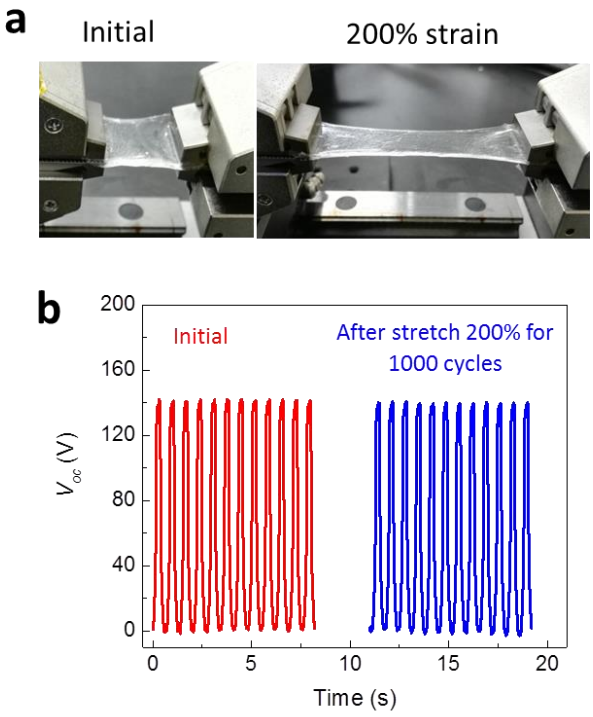

fig. S14. Stretching cycling test of the STENG. (**a**) The photo of a PDMS-STENG at initial state and 200% state. (**b**) The comparison of the output V_{oc} of the PDMS-STENG before and after stretching 200% for 1000 cycles.

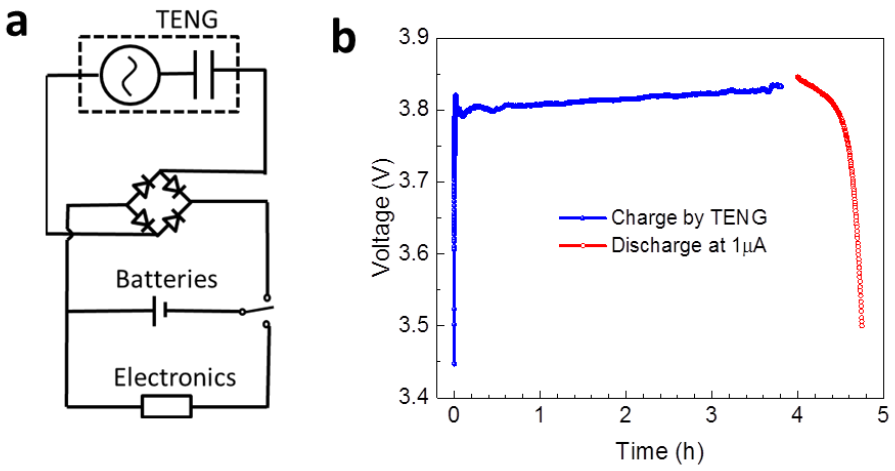

fig. S15. Battery charging by the STENG. (**a**) The equivalent circuit of a self-charging system by using the energy generated from the STENG to charge batteries and power electronics. The STENG is working at two-electrode mode. (**b**) The voltage profile of a $LiCoO_2$-Li battery ($LiCoO_2$ as the cathode, Li metal as the anode) charged by a PDMS-STENG at two-electrode mode with relative contact-separation motion to an Al metal film, and discharged by a constant current of 1 μA for 45 min. Before the battery charging by the STENG, the $LiCoO_2$-Li battery was discharged to 3.5 V at a current of 1 μA repeatedly for three times to deplete the residual capacity.

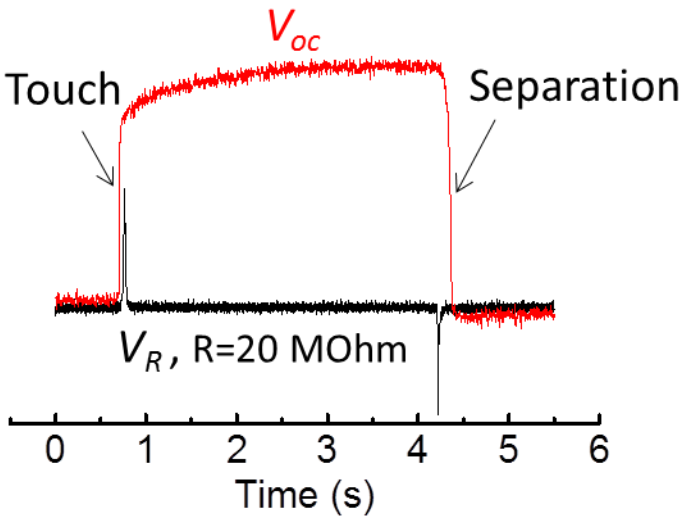

fig. S16. The difference between the V_{OC} and the voltage across the resistor.

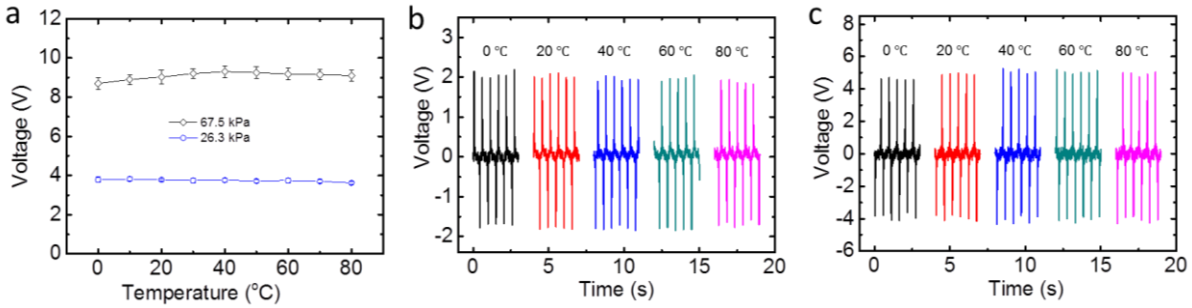

fig. S17. Temperature effect on the sensing properties of the STENG. (**a**) Summarized voltage across the resistor measured at different temperatures. The touch pressure are 67.5 kPa and 26.3 kPa, respectively. The voltage profiles of the (**b**) 26.3 kPa and (**c**) 67.5 kPa at different temperatures.

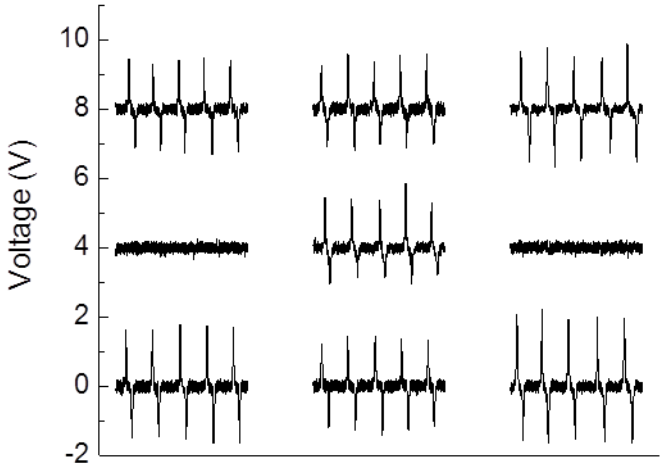

fig. S18. Voltages of the 9 pixels when pressing the sensor matrix with a z-shaped acrylic plate.

movie S1. Hand-tapping energy harvesting of a VHB-STENG at initial state.

movie S2. Hand-tapping energy harvesting of a VHB-STENG at stretched state.

movie S3. Powering an LCD screen by a transparent VHB-STENG.

movie S4. Powering an electronic watch with the energy converted from hand tapping by a PDMS-STENG.